



Effect of surfactants on Pb(II) adsorption from aqueous solutions using oxidized multiwall carbon nanotubes

Jiaying Li^{a,*}, Shuyu Chen^b, Guodong Sheng^a, Jun Hu^a, Xiaoli Tan^a, Xiangke Wang^{a,**}

^a Key Laboratory of Novel Thin Film Solar Cells, Institute of Plasma Physics, Chinese Academy of Sciences, P.O. Box 1126, 230031 Hefei, PR China

^b Nano Science and Nano Technology Program, The Hong Kong University of Science and Technology, Clear Water Bay, Kowloon, Hong Kong

ARTICLE INFO

Article history:

Received 8 September 2010

Received in revised form 4 November 2010

Accepted 4 November 2010

Keywords:

OMWCNTs
Adsorption
Pb(II)
Surfactants
pH

ABSTRACT

Batch experiments were conducted to elucidate the adsorption of Pb(II) and three types of widely used surfactants (sodium dodecylbenzene sulfonate (SDBS), octyl-phenol-ethoxylate (TX-100), and benzalkonium chloride (BKC)) from aqueous solutions by using oxidized multiwall carbon nanotubes (OMWCNTs). The effect of each kind of surfactant on the adsorption of Pb(II) and vice versa were studied in detail. The results indicated that the pH values affected the adsorption of Pb(II), TX-100 and BKC to OMWCNTs dramatically, whereas the adsorption of SDBS was almost pH-independent at pH < 9 and then decreased with increasing pH at pH > 9. The adsorption of Pb(II) was enhanced obviously by the presence of SDBS, but slightly inhibited by the presence of BKC. The adsorption of Pb(II) can be well described by Langmuir model. The adsorption process in the Pb–surfactant–OMWCNT ternary system was attributed to electrostatic, hydrophobic and π – π interactions. XPS analysis showed that the adsorption mechanism was mainly due to chemical interaction between Pb(II) and the surface functional groups of OMWCNTs and the surfactants.

© 2010 Elsevier B.V. All rights reserved.

1. Introduction

Surfactants have complex effects on the behavior of other contaminants by solubilization, catalysis [1], interfere in the removal processes of insoluble/soluble substances [2–4], and also can improve the dispersion of nanoparticles [3]. To date many publications have studied the dispersion effect of OMWCNTs caused by surfactant [5,6] and the adsorption isotherm appears on particles charged oppositely to the surfactant, or, in the case of nonionic surfactants, on particles with hydrogen bonding sites on the surface [7]. Surfactants have many uses in chemical industry, but can also form large foam masses, impact on aquatic organisms, causes serious pollution problems with considerable amounts released to the environment.

Lead is toxic for living species at some concentrations and it is a serious public health issue worldwide. Long-term drink of water at high lead level will cause anemia, headache, chills, diarrhea and poisoning leading to the dysfunction of kidneys, reproductive system, liver, brain and central nervous system [8]. When the surfactants and lead coexist in the environment, it is possibly much more detrimental to living species because of the multiple toxicities of lead, surfactants and the complexation compounds of them.

Due to the extremely porous and hollow structure, high specific surface area, and light mass density, CNTs [9] can be used as adsorbents for pollutant preconcentration for environmental remediation purposes. CNTs are found efficient for the removal of toxic substances such as organic contaminants [10–13] and various metal ions [14–19]. With increasing production and application of CNTs, it is necessary to understand the interaction between CNTs and heavy metal ions in the presence of surfactants. However, few studies have been conducted to systematically investigate the adsorption mechanisms of heavy metal ions to CNTs in the presence of surfactants [20–22], compared with the extensive studies on the adsorption of ether heavy metal ions or surfactants to CNTs. The coexistence of heavy metal ions and surfactants in the industrial wastewater further makes this an emergent topic. It should be realized that the presence of heavy metal ions affects the adsorption of surfactants from wastewaters, and vice versa. Thereby, it is very important to study the adsorption behaviors of heavy metal ions in the presence of different surfactants. However, to the best of our knowledge, no literature is available to understand the role of different surfactants on the adsorption of Pb(II) on CNTs. Recently we studied the adsorption of copper(II) on CNTs in the absence/presence of humic or fulvic acids [23] and ionizable aromatic compounds on as-prepared and oxidized CNTs [24]. In this paper, we reported the effect of three normal types of surfactants (sodium dodecylbenzene sulfonate (SDBS), octyl-phenol-ethoxylate (TX-100), and benzalkonium chloride (BKC)) on the adsorption of Pb(II) by using oxidized multiwall carbon

* Corresponding author.

** Corresponding author. Tel.: +86 551 5592788; fax: +86 551 5591310.

E-mail addresses: lijx@ipp.ac.cn (J. Li), xkwang@ipp.ac.cn (X. Wang).

nanotubes (OMWCNTs). A possible adsorption mechanism is also proposed.

2. Materials and methods

2.1. Preparation and oxidation of MWCNTs

MWCNTs, with outer diameter of 10–30 nm and length of about 30 μm , were prepared by using chemical vapor deposition (CVD) of acetylene in hydrogen flow at temperature of 760 °C using Ni–Fe nanoparticles as catalysts. $\text{Fe}(\text{NO}_3)_2$ and $\text{Ni}(\text{NO}_3)_2$ were treated by sol–gel process and calcinations to get FeO and NiO and then reduced by H_2 to get Fe and Ni nanoparticles. The as-grown MWCNTs were oxidized by using 3 mol/L HNO_3 to remove the hemispherical caps and to generate functional groups on the nanotubes. The mixture of 3 g MWCNTs and 400 mL 3 mol/L HNO_3 was ultrasonically stirred for 24 h. The suspension was filtrated and then rinsed with deionized water until the pH of the suspension reached about 6, and dried at 80 °C. Thus prepared OMWCNTs were calcined at 450 °C for 24 h to remove the amorphous carbon, and used in the following experiments. Using N_2 -BET method, the specific surface area of the OMWCNTs was 197 m^2/g . The point of zero charge, pH_{pzc} , i.e., the pH above which the total surface of the OMWCNTs is negatively charged, was measured at $\text{pH} \sim 5$. [18]

2.2. Preparation of Pb(II) stock solution

Analytical-grade lead nitrate was employed to prepare a stock solution containing 4.83 mmol/L of Pb(II) by dissolving $\text{Pb}(\text{NO}_3)_2$, which was further diluted with deionized water to the required Pb(II) concentrations in the adsorption experiments.

2.3. Surfactants

Three types of surfactants (i.e., SDBS with a purity of 95%, TX-100 with a purity of 95%, and BKC with a purity of 95%) were purchased from Shanghai Chemical Reagent Co., Ltd. (China). Their average molecular weights are 348.48, 646.86, and 368.04 g/mol, respectively. Their chemical formulas are $\text{CH}_3(\text{CH}_2)_{11}\text{C}_6\text{H}_4\text{SO}_3^- \text{Na}^+$, $\text{C}_8\text{H}_{17}\text{C}_6\text{H}_4\text{O}(\text{CH}_2\text{CH}_2\text{O})_{10}\text{H}$, and $\text{C}_6\text{H}_5\text{CH}_2\text{N}^+(\text{CH}_3)_2(\text{CH}_2)_{13}\text{CH}_3\text{Cl}^-$, respectively. The critical micelle concentration (CMC) at 298 K are 1.41 mmol/L [3], 0.27 mmol/L [3], and 2.0 mmol/L [25,26], respectively. The stock solution containing 10 mmol/L of surfactant was further diluted with deionized water to the required surfactant concentrations in the adsorption measurements.

2.4. Batch experiments

The adsorption of Pb(II) and surfactants on OMWCNTs was investigated by using batch technique in 10 mL polyethylene centrifuge tube. The concentration of OMWCNTs stock suspension is 3.0 g/L and NaCl is 0.1 M. Certain amount of stock suspension of OMWCNTs and NaCl were pre-equilibrated for 24 h, and then Pb(II) stock solution was added to achieve the desired concentrations of the different components. For example, to obtain the sample (initial Pb(II) concentration = 0.0483 mmol/L, initial surfactant concentration = 0.83 mmol/L, adsorbent dosage = 0.75 g/L, $I = 0.01$ mol/L NaCl), 1.5 mL 3.0 g/L OMWCNTs solution, 0.6 mL 0.1 M NaCl solution and 2.4 mL deionized water were added and pre-equilibrated for 24 h, and then 1.0 mL Pb(II) stock solution was added. The system was adjusted to the desired pH by adding negligible volumes of 0.01 or 0.1 mol/L HCl or NaOH. After the suspensions were sonicated with a sonicator for 0.5 h at 128 W and shaken for 2 days, the solid and liquid phases were separated by ultracentrifugation at 18,000 rpm for 30 min and filtration by using

0.45 μm membrane filter. The adsorbed amounts of Pb(II) was calculated from the difference between the initial concentration and the equilibrium one. The concentration of Pb(II) was analyzed by spectrophotometry at wavelength of 616 nm by using Pb CAP-III complex.

To investigate the adsorption of SDBS, TX-100 and BKC on OMWCNTs, experiments were carried out as follows: OMWCNTs and NaCl were pre-equilibrated for 24 h, then SDBS, TX-100 or BKC were added and the pH was adjusted as in the Pb(II) adsorption process. Samples were sonicated with a sonicator for 0.5 h at 128 W and then gently shaken for 2 days. The SDBS, TX-100 and BKC concentrations in supernatant were determined at 260.8 nm, 277.0 nm, and 262.0 nm with ultraviolet–visible (UV–vis) spectrophotometry, respectively. Duplicate batches were examined to prepare adsorption curves and the relative errors of the data were about 5%.

2.5. Spectroscopic analysis

For the XPS analysis, the samples were equilibrated for 2 days and then filtrated and washed with blank electrolyte to remove unbound SDBS, TX-100 or BKC and Pb(II), and then the samples were dried at 60 °C. XPS data were obtained with an ESCALab220i-XL electron spectrometer from VG Scientific using 300 W Al $K\alpha$ radiation. The pressure in the analysis chamber was maintained below 3×10^{-9} mbar. The XPS photoelectron binding energies (BE) of the adventitious carbon species, i.e., the C 1s line at 284.8 eV, was used to correct the observed BE for surface charging [27].

3. Results and discussion

3.1. Effect of pH

The adsorption percentage of Pb(II) from aqueous solution on OMWCNTs as a function of pH in the presence of different surfactants are shown in Fig. 1a. The adsorption percentage is calculated using the following equation:

$$\text{Removal\%} = \frac{C_0 - C_e}{C_0} \times 100\% \quad (1)$$

where C_0 (mol/L) is the initial Pb(II) concentration, C_e (mol/L) is the concentration in supernatant after ultrafiltration. As can be seen from Fig. 1a, the adsorption of Pb(II) to OMWCNTs is strongly dependent on pH values. The adsorption percentage of Pb(II) increases very quickly from about 17% to 85% at pH range of 4–7, maintains level with increasing pH values at pH 7–10, and then decreases steeply to about 30% at $\text{pH} > 12$ in the absence of surfactants. In the presence of SDBS, the adsorption of Pb(II) increases from 63% to 95% at pH ranging from 4 to 7, maintains the high level with increasing pH values at pH range of 7–11, and then decreases slowly down to 75% at $\text{pH} > 12$. The presence of TX-100 slightly increases the adsorption of Pb(II) at $\text{pH} < 7$ as compared to the adsorption of Pb(II) on bare OMWCNTs. It is interesting to note that the influence of SDBS on Pb(II) adsorption is much higher than that of TX-100 or BKC, which may be interpreted by the formation of complex compounds between divalent cation ions (Pb^{2+}) and the anionic surfactant (DBS^-).

It is known that Pb(II) ions present in the forms of Pb^{2+} , $\text{Pb}(\text{OH})^+$, $\text{Pb}(\text{OH})_2^0$, and $\text{Pb}(\text{OH})_3^-$ at different pH values (table of equilibrium constants and figure of distribution of Pb(II) species as a function of pH are listed in Supplementary Material) [28–30]. At $\text{pH} < 6$, the predominant species is Pb^{2+} and the adsorption of Pb^{2+} is mainly accomplished by adsorption reaction. Therefore, the low Pb^{2+} adsorption that takes place at low pH can be attributed partly to the competition between H^+ and Pb^{2+} ions on the surface sites [31]. In the pH range of 7–10, the adsorption of Pb(II) remains constant and reaches maximum. The main species of Pb(II) at pH 7–10

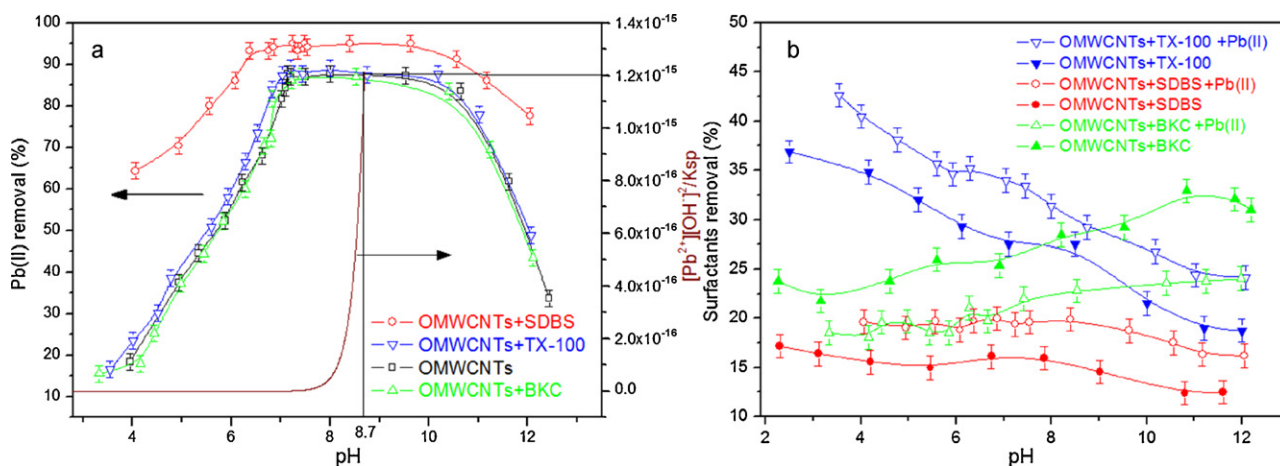


Fig. 1. Effect of pH on the adsorption of Pb(II) to OMWCNTs as a function of pH (a), and effect of pH on the adsorption of different surfactants to OMWCNTs in the presence and absence of Pb(II) ions as a function of pH (b). Initial Pb(II) concentration = 0.0483 mmol/L, initial surfactant concentration = 0.83 mmol/L, adsorbent dosage = 0.75 g/L, $I = 0.01$ mol/L NaCl, $T = 25 \pm 1$ °C.

are $Pb(OH)^+$ and $Pb(OH)_2^0$. Thus the adsorption of Pb(II) is possibly accomplished by simultaneous precipitation of $Pb(OH)_2^0$ and adsorption of $Pb(OH)^+$. The $Pb(OH)_3^-$ species are predominated gradually at $pH > 10$; therefore, the decrease in Pb(II) adsorption to OMWCNTs at pH 10–12 can be attributed to the electrostatic repulsion. The negative charged $Pb(OH)_3^-$ is difficult to be adsorbed on the negatively charged surface of OMWCNTs at high pH values [32]. The precipitation curve of Pb(II) at the concentration of 4.83×10^{-5} mol/L is also shown in Fig. 1a. The precipitation constant of $Pb(OH)_2(s)$ is 1.2×10^{-15} . It is clear that Pb(II) begins to form precipitation at pH 8.7 if no Pb(II) is adsorbed on OMWCNTs. However, >80% Pb(II) is adsorbed on OMWCNTs at pH 7, it is impossible to form precipitation because of the very low concentration of Pb(II) remained in solution. The high adsorption of Pb(II) on the surfaces of OMWCNTs can result in the high concentration of Pb(II) at local areas and can form precipitates on the surfaces of OMWCNTs. Therefore, the abrupt adsorption of Pb(II) on OMWCNTs at pH 6–7 is not only attributed to the precipitation of $Pb(OH)_2$ but also to the surface complexation of Pb(II) with functional groups on OMWCNTs. The species of Pb(II) in solution at different pH values determine the adsorption of Pb(II) from aqueous solution to OMWCNTs. From the results, one can see that the best pH range for the removal of Pb(II) from solution by using OMWCNTs is 7–10.

The adsorption percentage of different surfactants to OMWCNTs as a function of pH in the presence/absence of Pb(II) is shown in Fig. 1b. The adsorption of SDBS maintains level at low pH and decreases slightly at $pH > 9$. The adsorption of TX-100 decreases with increasing pH values from 3 to 12, whereas that of BKC increases with increasing pH values. The negative charged density of OMWCNTs increases with increasing pH values [17,19], which reinforce the electrostatic attraction between OMWCNTs and BKC with positive charge, the electrostatic repulsion between OMWCNTs and negatively charged head-group of SDBS. The main surface species on OMWCNTs are $-COOH$ and $-OH$ groups. At low pH, they can form hydrogen bindings with oxyethyl groups of TX-100 [16], while at high pH, the $-COOH$ groups will become $-COO^-$ through losing its H^+ , reducing the number of hydrogen bindings. The decrease in adsorption of TX-100 can therefore be explainable on this basis.

3.2. Effect of surfactants on Pb(II) adsorption

Fig. 2a shows the adsorption percentage of Pb(II) from aqueous solution to OMWCNTs as a function of initial surfactant concentrations at $pH = 4.1 \pm 0.1$ and in 0.01 M NaCl solutions. The adsorption of Pb(II) increases from ~17% to ~22% with increasing TX-100

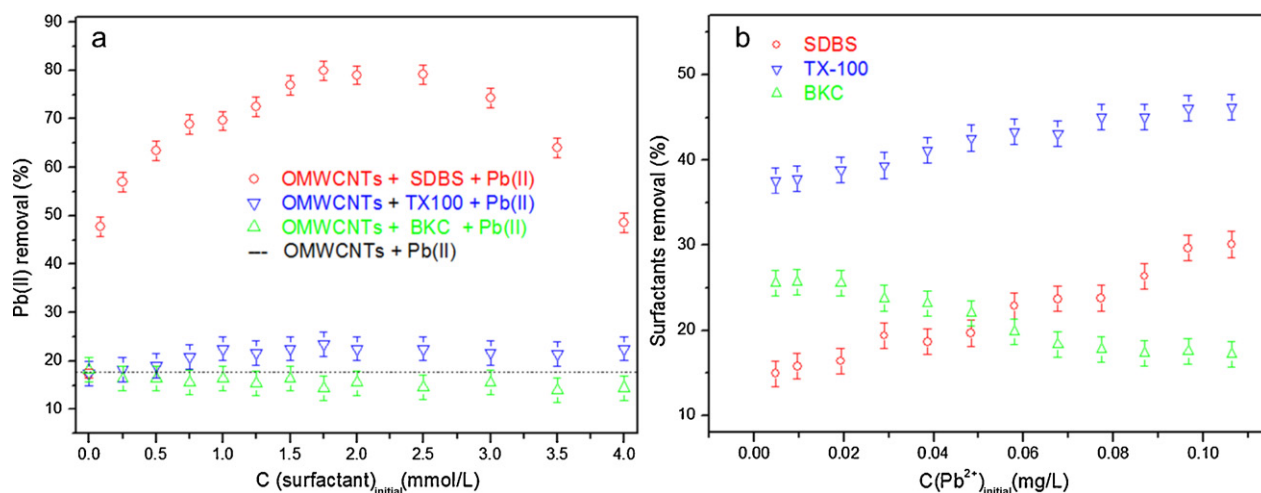


Fig. 2. Effect of surfactant concentrations on the adsorption of Pb(II) to OMWCNTs (a), initial Pb(II) concentration = 0.0483 mmol/L. The dash line represents the sorption of Pb(II) in the absence of surfactants; Effect of Pb(II) concentrations on the adsorption of surfactants to OMWCNTs (b), initial surfactant concentration = 0.83 mmol/L. Adsorbent dosage = 0.75 g/L, $pH = 4.1 \pm 0.1$, $I = 0.01$ mol/L NaCl, $T = 25 \pm 1$ °C.

concentration from 0 to ~2.0 mmol/L, and then maintains level with increasing TX-100. Whereas the adsorption of Pb(II) decreases slightly from ~17% to ~13% with increasing BKC concentration from 0 to ~2.0 mmol/L, and then maintains level with increasing BKC concentrations in the OMWCNTs suspension. However, the presence of SDBS enhances Pb(II) adsorption dramatically. The adsorption of Pb(II) increases to maximum (~80%) at SDBS concentration about 2.0 mmol/L, then decreases to ~45% when the SDBS concentration increases to 4.0 mmol/L.

The main effect of SDBS on Pb(II) adsorption is possibly attributed to the formation of complex compound $Pb(DBS)_2$ between divalent cation and the anionic surfactant (DBS^-) [33]. The adsorption percentage of Pb(II) increases sharply to maximum at the initial concentration of SDBS about 2.0 mmol/L and then decreases to about 45% when SDBS concentration increases to 4.0 mmol/L. SDBS begins to form aggregation [30] if the concentration is higher than the CMC (1.41 mmol/L) [3]. At the CMC of SDBS, the micelles begin to form in aqueous solutions, and the complex compound of $Pb(DBS)_2$ decrease with increasing SDBS concentration, which is primarily due to the counterion binding of Pb(II) into any micelles. Another minor possible interaction is attributed to the formation of cation-SDBS complex compounds on the accessible sorption sites on OMWCNTs surfaces. The coating of OMWCNTs by SDBS may lead to the modification of the surfaces and the partial complexation of Pb(II) with SDBS adsorbed on OMWCNTs increases Pb(II) sorption [34,35].

Surfactants can form admicelles, hemimicelles or micelles and affect the adsorption of other adsorbate on solid surface [36]. When the surfactant concentration is 0.83 mmol/L, BKC or SDBS may form admicelle (or hemimicelles) on OMWCNT surfaces. There is competition between the adsorption of BKC admicelles and Pb(II). The negative charged SDBS admicelles, on the other hand, promote the adsorption of Pb(II). However, the concentration of TX-100 is far above its CMC (0.27 mmol/L), and can form much more micelles in aqueous solution. Therefore its adsorption on OMWCNTs can be affected deeply by pH and Pb(II).

3.3. Effect of Pb(II) on surfactants adsorption

Fig. 2b shows the adsorption of different surfactants to OMWCNTs as a function of initial Pb(II) concentrations at pH 4.1 ± 0.1 in 0.01 M NaCl solutions. The adsorption percentage of SDBS and TX-100 from solution to OMWCNTs increases from ~15% to ~30%, and from ~38% to ~47%, respectively, with initial Pb(II) concentrations increasing from 0 to 10.8 mmol/L. However, the adsorption of BKC decreases slightly with initial Pb(II) concentrations increasing from 0 to 10.8 mmol/L. The effects of Pb(II) concentrations on the adsorption of surfactant to OMWCNTs are attributed to the complex and electrostatic interactions among surfactants, Pb(II) and functional groups of OMWCNTs, and will be discussed in detail in the section of the adsorption mechanism.

3.4. Sorption isotherms

The sorption isotherms of Pb(II) in the presence of different surfactants on OMWCNTs at pH 4.1 ± 0.1 and in 0.01 M NaCl solu-

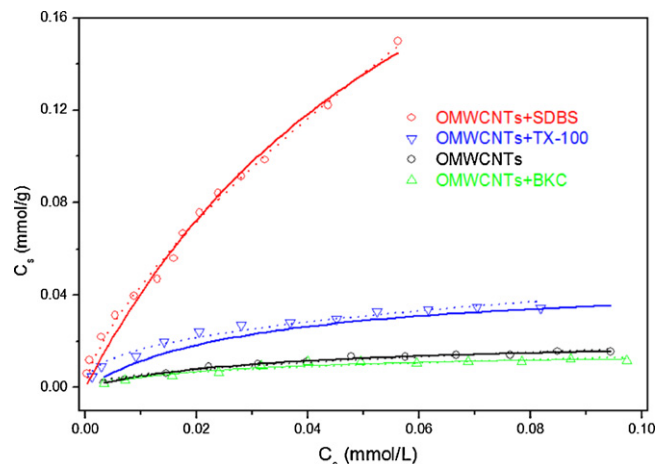


Fig. 3. Sorption isotherms of Pb(II) to OMWCNTs. Adsorbent dosage = 0.75 g/L, initial surfactant concentration = 0.83 mmol/L, pH = 4.1 ± 0.1 , $I = 0.01$ mol/L NaCl, $T = 25 \pm 1$ °C. Solid line: Langmuir model, dash line: Freundlich model.

tions are shown in Fig. 3. In order to gain a better understanding of the mechanism and to quantify the sorption data, Langmuir ($C_s = a b C_e / (1 + b C_e)$) and Freundlich ($C_s = K_f C_e^{1/n}$) isotherm models [28,37] are conducted to simulate the sorption of Pb(II) on OMWCNTs. Herein, a is the maximum sorption capacity; b is the Langmuir sorption constant; and K_f and $1/n$ are the Freundlich constants. The Langmuir and Freundlich constants obtained by fitting the sorption equilibrium data are listed in Table 1. The values of correlation coefficient (R^2) derived from Langmuir model are much closer to 1 than those derived from Freundlich model, which indicates that the sorption of Pb(II) on OMWCNTs is simulated better by Langmuir model than by Freundlich model. One can see that the sorption percentages of Pb(II) on OMWCNTs under the same Pb(II) initial concentration are in the following sequence: SDBS > TX-100 > No surfactants > BKC, indicating that the surfactant can alter the surface property of OMWCNTs and thus can influence the sorption of Pb(II) on OMWCNT surface.

3.5. Schematic adsorption mechanism

3.5.1. Pb(II)–SDBS–OMWCNTs system

Based on the results mentioned above, the schematic possible adsorption mechanisms of Pb(II) and surfactants to OMWCNTs are shown in Fig. 4. It is commonly believed that the chemical interaction and electrostatic attraction between Pb(II) and the surface functional groups of OMWCNTs are the major adsorption mechanisms (part c in Fig. 4). The adsorption of metal ions on OMWCNTs is mainly attributed to surface complexation, ion exchange and electrostatic attraction [18,19,38]. In the presence of SDBS, OMWCNT surface becomes hydrophilic due to SDB-group of the surfactants oriented toward the bulk solution, which can provide more functional sites to bond metal ions at OMWCNT surface [39]. A small quantity of SDBS molecules adsorbed on the surfaces of OMWCNTs causes the interaction between the anionic head groups and the positive charged cation ions, and thereby promotes the sorp-

Table 1
Parameter of sorption models for Pb(II) on OMWCNTs.

System	Langmuir model			Freundlich model		
	a (mmol/g)	b (L/mmol)	R^2	K_f (mmol/g)	$1/n$	R^2
OMWCNTs + Pb	0.0211	30.56	0.9899	0.0527	0.49	0.9629
OMWCNTs + TX-100 + Pb	0.0414	65.34	0.9848	0.0994	0.39	0.9694
OMWCNTs + BKC + Pb	0.0158	38.29	0.9564	0.0367	0.44	0.9027
OMWCNTs + SDBS + Pb	0.3231	14.46	0.9853	1.1040	0.70	0.9945

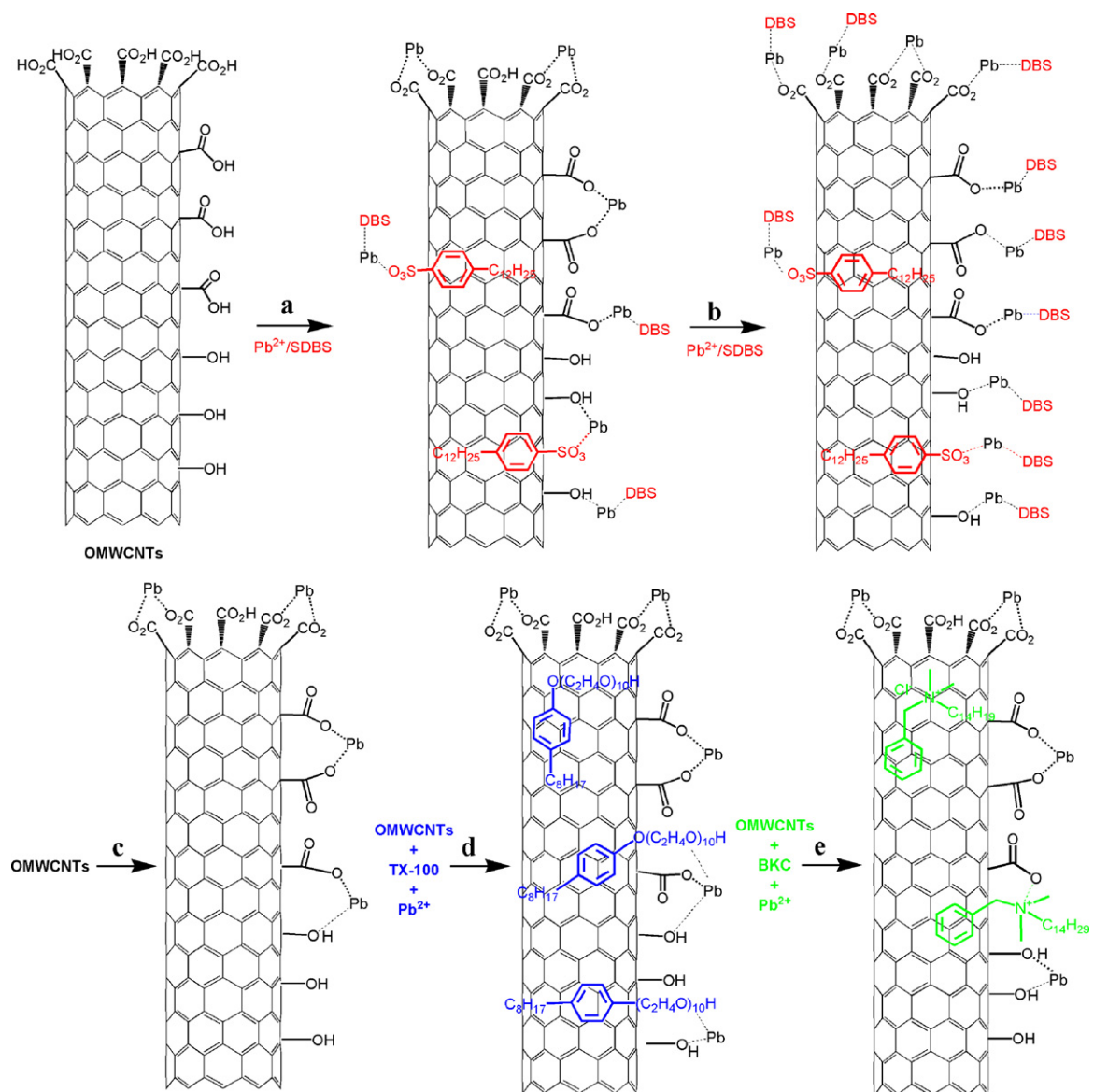


Fig. 4. Diagram of the possible mechanisms for adsorption of Pb(II) and surfactants on OMWCNTs.

Table 2
Measured binding energies (BE) and full widths at half maximum (FWHM) of XPS analysis.

Sample	Signal	Peak	BE (eV)	FWHM (eV)
OMWCNTs–Pb	O 1s	C–O	533.1	1.76
		O–C=O	531.7	1.56
		Pb–O	530.9	1.56
		Pb–R	138.80	1.29
OMWCNTs–SDBS–Pb	O 1s	(R functional groups)	143.68	1.26
		C–O	533.1	1.97
		O–C=O	531.7	0.94
		Pb–O	530.9	1.14
OMWCNTs–TX-100–Pb	O 1s	O–S=O	532.0	1.29
		Pb–R	138.85	1.40
		(R functional groups)	143.74	1.24
		C–O	533.1	1.59
OMWCNTs–BKC–Pb	O 1s	O–C=O	531.8	1.49
		Pb–O	531.0	1.19
		Pb–R	138.78	1.31
		(R functional groups)	143.73	1.26
OMWCNTs–BKC–Pb	O 1s	C–O	533.0	1.8
		O–C=O	532.2	2.3
		Pb–O	530.9	1.4
		Pb–R	138.70	1.32
OMWCNTs–BKC–Pb	Pb 4f	(R functional groups)	143.61	1.18

tion of Pb(II) to OMWCNTs slightly (part a in Fig. 4). The adsorption of Pb(II) on the surfaces of OMWCNTs increases with increasing SDBS concentrations, which results in the increasing of the coordination sites of Pb(II) with DBS⁻ groups. Thereby, the adsorption of SDBS increases with increasing Pb(II) concentrations (part b in Fig. 4).

3.5.2. Pb(II)–TX-100–OMWCNTs system

A number of the possible mechanisms that may be responsible for enhanced adsorption of TX-100 in the presence of Pb(II) are discussed: (i) Surface complex formation of Pb(II) on the surfaces of OMWCNTs changes the properties of OMWCNTs, which further affects the adsorption of TX-100 on the negatively charged sur-

faces of OMWCNTs. The surface charge has a marked influence on the adsorption of TX-100 from the solution phase. The increasing negative surface charge decreases the adsorption of TX-100 and increases the adsorption of Pb(II) on OMWCNTs. When Pb(II) is adsorbed on OMWCNTs, the surface charge of OMWCNTs is less negative; thus, more TX-100 is adsorbed on OMWCNTs. (ii) Cationic Pb(II) and TX-100 are likely to form complexes, and these complexes may facilitate the adsorption of TX-100 on the surfaces of OMWCNTs. The strong donor sites of TX-100 may be the oxygen atoms of the ether groups in the molecule of TX-100 (part d in Fig. 4), which is an effective target of Pb–TX-100 complexes. When compared with TX-100, the Pb(II)–TX-100 complex is less negatively charged, which decreases the repulsive electrostatic forces

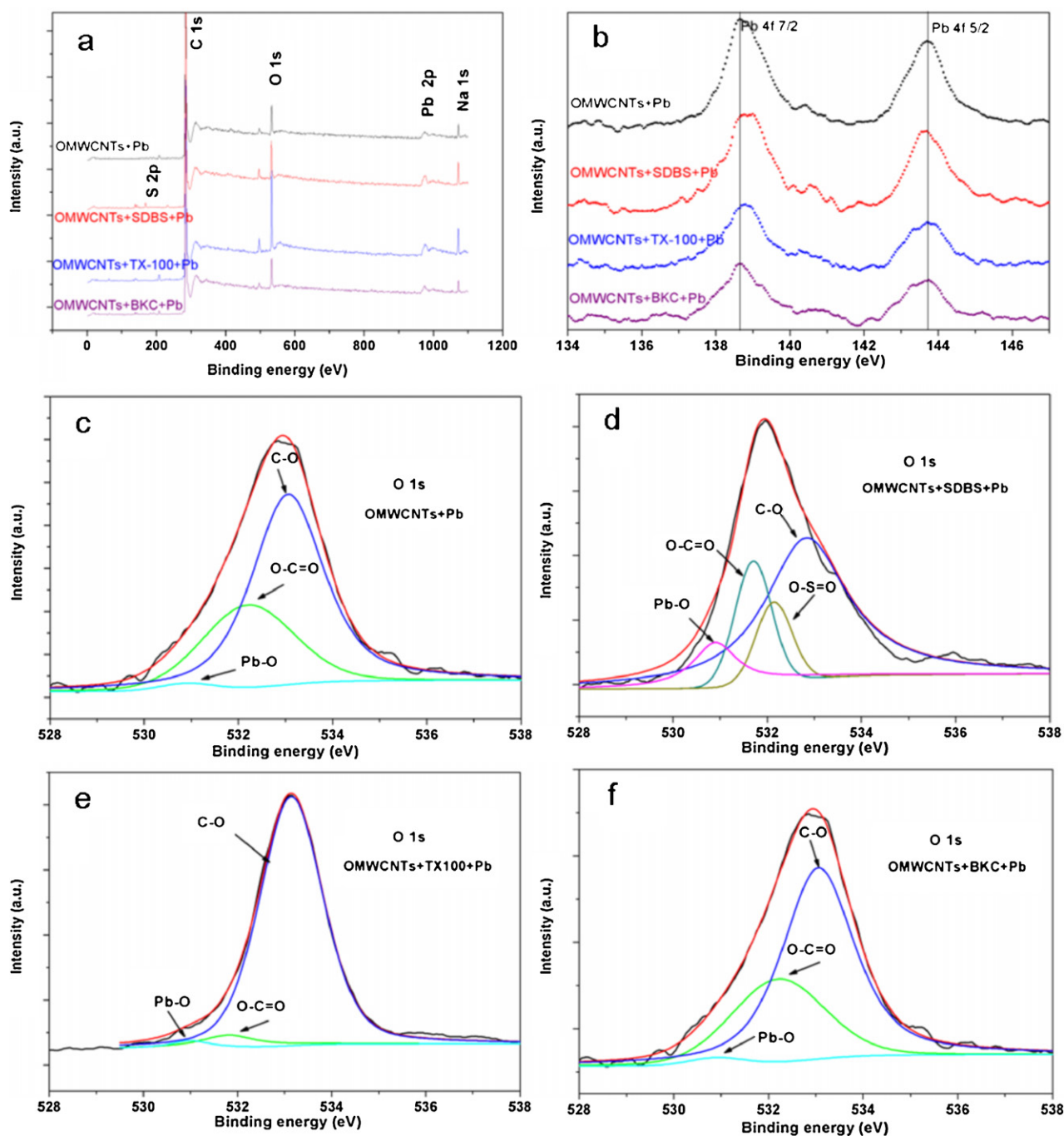


Fig. 5. XPS wide-scan (a), Pb 2p (b), and O 1s high-resolution spectra of OMWCNTs–Pb (c), MWCNTs–SDBS–Pb (d), MWCNTs–TX-100–Pb (e), and MWCNTs–BKC–Pb (f).

between TX-100 and the negatively charged OMWCNTs, facilitating the adsorption of TX-100 on OMWCNTs.

From the part d in Fig. 4, it can be seen that not only functional groups of OMWCNTs but also some oxygen atoms of TX-100 adsorbed on the surfaces of OMWCNTs participate in chemi-complexation with Pb(II), which increases slightly the adsorption of Pb(II) from aqueous solutions.

3.5.3. Pb(II)–BKC–OMWCNTs system

The competitive adsorption is the possible mechanism of Pb(II) and BKC adsorption on OMWCNTs. As mentioned above, the formation of surface complexes of Pb(II) results in the surface of OMWCNTs less negative, which subsequently has a lower affinity for the adsorption of cationic surfactant BKC through cation exchange. BKC may interact with functional groups on the surfaces of OMWCNTs and then is adsorbed on OMWCNTs (part e in Fig. 4). The adsorption of BKC also makes the surfaces of OMWCNTs less negative and inhibits slightly the adsorption of Pb(II) on BKC bound OMWCNTs. The negative charged density of OMWCNTs increases with increasing pH values [14], which reinforces the electrostatic attraction between negative charged OMWCNTs and positive charged BKC. It is an interaction of reciprocal inhibition in the adsorption of BKC and Pb(II) from the aqueous solutions to OMWCNTs.

3.6. XPS analysis

In order to get the information of Pb(II) adsorption on OMWCNTs at molecular level, a complementary description of the systems have been obtained by XPS analysis to identify the Pb(II) species adsorbed on OMWCNTs and SDBS, TX-100, BKC bound OMWCNTs. Typical XPS survey spectra are shown in Fig. 5a. Peaks are present for the expected components of OMWCNTs and two small but clear peaks appear at BE typical for Pb 4f. The peaks suggest the most significant amount of Pb(II) adsorbed on OMWCNTs. The adsorbed Pb(II) can be readily identified by the Pb 4f_{7/2} and Pb 4f_{5/2} XPS lines (Fig. 5b). Photoelectron energies are sensitive to the local binding environments. Compared to others, a shift (about 0.5 eV) can be clearly seen in the Pb–SDBS–OMWCNT system, which is attributed to the binding of Pb ions on the surfaces of OMWCNTs through the functional groups of SDBS adsorbed on OMWCNTs. As regarded the Pb 4f peak (Fig. 5b), only divalent states of Pb components and the associated satellites are detected in these spectra [28]: a signal located at a BE of 138.8 eV (with a satellite at 143.7 eV with respect to the main signal in Table 2 may be due to the formation of Pb–O bond between Pb(II) and functional groups R (R represents the functional groups of –CO, –COO, –SO₃).

The Pb 4f_{7/2} peak at 138.8 eV in the Pb–OMWCNTs system can be attributed to the reaction of Pb with functional groups on the surfaces of OMWCNTs. While in the Pb–SDBS–OMWCNTs system, the shift of BE of Pb(II) to higher energy sides indicates that the interactions of Pb–SDBS–OMWCNTs are stronger than those of others. These shifts in both Pb 4f BE are also probably indicative of the partial of Pb(II) ions binding on the surfaces of OMWCNTs through the functional groups of SDBS adsorbed on OMWCNTs. These data help to explain the increase in the adsorption of Pb(II) on SDBS bound OMWCNTs. The coating of OMWCNTs by TX-100 and BKC leads to the modification of the surfaces and almost no contribution to Pb(II) adsorption.

Fig. 5c–f shows the high resolution O 1s spectra of Pb–OMWCNTs and Pb–SDBS–OMWCNTs. The O 1s spectrum of Pb–OMWCNTs (Fig. 5c) is resolved into three individual component peaks: O–C=O (531.7 eV), C–O group (533.1 eV) and adsorbed Pb–O (530.9 eV) group [28,40]. The O 1s spectrum of Pb–SDBS–OMWCNTs (Fig. 5d) is resolved into four individual com-

ponent peaks: the groups of O–C=O (531.7 eV), C–O (533.1 eV) and adsorbed O–Pb (530.9 eV) do not change, while the group of O–S=O (532.0 eV) appears due to the introduction of SDBS. While in the presence of TX-100 and BKC, the O 1s spectra (Fig. 5e and f) are also resolved into three individual component peaks, and the intensity of each peak is different from the Pb–OMWCNTs. The group of O–Pb indicates that Pb adsorbed on the surfaces of OMWCNTs is probably in the form of Pb–R (R represents functional groups of –CO, –COO). These species also indicate that the functional groups are introduced in the oxidation of OMWCNTs. The results are greatly in agreement with the earlier references of the XPS studies of Pb²⁺ adsorbed on OMWCNTs [28,41].

4. Conclusions

The adsorption of different surfactants on OMWCNTs plays an important role in Pb(II) adsorption process. The relationship between the adsorption property and the surface functional groups prove to be helpful for understanding the adsorption behavior of surfactants and Pb(II), and could be valuable for the treatment of heavy metal ions and surfactants polluted water. Surfactants and heavy metal ions can be removed and enriched by OMWCNTs simultaneously. These results will contribute to understand the adsorption behavior of OMWCNTs and other functionalized carbon materials with heavy metal ions and surfactants in the natural environmental systems.

Acknowledgements

Financial supports from the Knowledge Innovation Program of CAS (085FCQ0121), National Natural Science Foundation (20907055; 20971126; 21077107) and 973 project (2007CB936602) are acknowledged.

Appendix A. Supplementary data

Supplementary data associated with this article can be found, in the online version, at doi:10.1016/j.cej.2010.11.018.

References

- [1] S.D. Haigh, A review of the interaction of surfactants with organic contaminants in soil, *Sci. Total Environ.* 185 (1996) 161–170.
- [2] M.J. Rosen, F. Li, S.W. Morrall, D.J. Versteeg, The relationship between the interfacial properties of surfactants and their toxicity to aquatic organisms, *Environ. Sci. Technol.* 35 (2001) 954–959.
- [3] Z.T. Han, F.W. Zhang, D.H. Lin, B.S. Xing, Clay minerals affect the stability of surfactant-facilitated carbon nanotube suspensions, *Environ. Sci. Technol.* 42 (2008) 6869–6875.
- [4] Z.M. Zheng, J.P. Obbard, Evaluation of an elevated non-ionic surfactant critical micelle concentration in a soil/aqueous system, *Water Res.* 36 (2002) 2667–2672.
- [5] M.F. Islam, E. Rojas, D.M. Bergey, A.T. Johnson, A.G. Yodh, High weight fraction surfactant solubilization of single-wall carbon nanotubes in water, *Nano Lett.* 3 (2003) 269–273.
- [6] Z.W. Wang, M.D. Shirley, S.T. Meikle, R.L.D. Whitby, S.V. Mikhailovsky, The surface acidity of acid oxidised multi-walled carbon nanotubes and the influence of in-situ generated fulvic acids on their stability in aqueous dispersions, *Carbon* 47 (2009) 73–79.
- [7] M.J. Rosen, *Surfactants and Interfacial Phenomena*, John Wiley & Sons, Inc., 2004, pp. 341–346.
- [8] C.K. Singh, J.N. Sahu, K.K. Mahalik, C.R. Mohanty, B.R. Mohan, B.C. Meikap, Studies on the removal of Pb(II) from wastewater by activated carbon developed from Tamarind wood activated with sulphuric acid, *J. Hazard. Mater.* 153 (2008) 221–228.
- [9] S. Iijima, Helical microtubes of graphitic carbon, *Nature* 354 (1991) 56–68.
- [10] C.S. Lu, Y.L. Chung, K.F. Chang, Adsorption thermodynamic and kinetic studies of trihalomethanes on multiwalled carbon nanotubes, *J. Hazard. Mater.* 138 (2006) 304–310.
- [11] K. Yang, X.L. Wang, L.Z. Zhu, B.S. Xing, Competitive sorption of pyrene, phenanthrene, and naphthalene on multiwalled carbon nanotubes, *Environ. Sci. Technol.* 40 (2006) 5804–5810.

- [12] K. Yang, L.Z. Zhu, B.S. Xing, Adsorption of polycyclic aromatic hydrocarbons by carbon nanomaterials, *Environ. Sci. Technol.* 40 (2006) 1855–1861.
- [13] K. Yang, B.S. Xing, Desorption of polycyclic aromatic hydrocarbons from carbon nanomaterials in water, *Environ. Pollut.* 145 (2007) 529–537.
- [14] C.S. Lu, H. Chiu, C.T. Liu, Removal of zinc(II) from aqueous solution by purified carbon nanotubes: kinetics and equilibrium studies, *Ind. Eng. Chem. Res.* 45 (2006) 2850–2855.
- [15] C.Y. Lu, H.S. Chiu, Adsorption of zinc(II) from water with purified carbon nanotubes, *Chem. Eng. Sci.* 61 (2006) 1138–1145.
- [16] P. Liang, Y. Liu, L. Guo, J. Zeng, H.B. Lu, Multiwalled carbon nanotubes as solid-phase extraction adsorbent for the preconcentration of trace metal ions and their determination by inductively coupled plasma atomic emission spectrometry, *J. Anal. Atom. Spectrom.* 19 (2004) 1489–1492.
- [17] Y.H. Li, Z.C. Di, J. Ding, D.H. Wu, Z.K. Luan, Y.Q. Zhu, Adsorption thermodynamic, kinetic and desorption studies of Pb^{2+} on carbon nanotubes, *Water Res.* 39 (2005) 605–609.
- [18] C.L. Chen, X.K. Wang, Adsorption of Ni(II) from aqueous solution using oxidized multiwall carbon nanotubes, *Ind. Eng. Chem. Res.* 45 (2006) 9144–9149.
- [19] X.K. Wang, C.L. Chen, W.P. Hu, A.P. Ding, D. Xu, X. Zhou, Sorption of $^{243}Am(III)$ to multi-wall carbon nanotubes, *Environ. Sci. Technol.* 39 (2005) 2856–2860.
- [20] Z.G. Pei, X.Q. Shan, B. Wen, B. He, T. Liu, Y.N. Xie, G. Owens, Sorption of anionic metsulfuron-methyl and cationic difenzoquat on peat and soil as affected by copper, *Environ. Sci. Technol.* 42 (2008) 6849–6854.
- [21] Y.J. Wang, D.A. Jia, R.J. Sun, H.W. Zhu, D.M. Zhou, Adsorption and cosorption of tetracycline and copper(II) on montmorillonite as affected by solution pH, *Environ. Sci. Technol.* 42 (2008) 3254–3259.
- [22] A. Karagunduz, Y. Kaya, B. Keskinler, S. Once, Influence of surfactant entrapment to dried alginate beads on sorption and removal of Cu^{2+} ions, *J. Hazard. Mater.* 131 (2006) 79–83.
- [23] G.D. Sheng, J.X. Li, D.D. Shao, J. Hu, C.L. Chen, Y.X. Chen, X.K. Wang, Adsorption of copper(II) on multiwalled carbon nanotubes in the absence and presence of humic or fulvic acids, *J. Hazard. Mater.* 178 (2010) 333–340.
- [24] G.D. Sheng, D.D. Shao, X.M. Ren, X.Q. Wang, J.X. Li, Y.X. Chen, X.K. Wang, Kinetics and thermodynamics of adsorption of ionizable aromatic compounds from aqueous solutions by as-prepared and oxidized multiwalled carbon nanotubes, *J. Hazard. Mater.* 178 (2010) 505–516.
- [25] J.R. Rodriguez, J. Czapkiewicz, Conductivity and dynamic light-scattering studies on homologous alkylbenzyltrimethylammonium chlorides in aqueous solutions, *Colloids Surf. A* 101 (1995) 107–111.
- [26] A. Makayssi, R. Bury, C. Treiner, Thermodynamics of micellar solubilisation for 1-pentanol in weakly interacting binary cationic surfactant mixtures at 25-degrees-C, *Langmuir* 10 (1994) 1359–1365.
- [27] E. Magnano, S. Vandre, J. Kovac, E. Narducci, R. Caloi, P. Manini, M. Sancrotti, Surface and subsurface properties of a $BaLi_4$ gettering alloy studied using X-ray photoemission spectroscopy, *Surf. Sci.* 404 (1998) 223–226.
- [28] D. Xu, X.L. Tan, C.L. Chen, X.K. Wang, Removal of Pb(II) from aqueous solution by oxidized multiwalled carbon nanotubes, *J. Hazard. Mater.* 154 (2008) 407–416.
- [29] G.D. Sheng, S.W. Wang, J. Hu, Y. Lu, J.X. Li, Y.H. Dong, X.K. Wang, Adsorption of Pb(II) on diatomite as affected via aqueous solution chemistry and temperature, *Colloids Surf. A* 339 (2009) 159–166.
- [30] J. Hu, D.D. Shao, C.L. Chen, G.D. Sheng, J.X. Li, X.K. Wang, M. Nagatsu, Plasma-induced grafting of cyclodextrin onto multiwall carbon nanotube/iron oxides for adsorbent application, *J. Phys. Chem. B* 114 (2010) 6779–6785.
- [31] F. Esmadi, J. Simm, Sorption of cobalt(II) by amorphous ferric hydroxide, *Colloids Surf. A* 104 (1995) 265–270.
- [32] I. Langmuir, The adsorption of gases on plane surface of glass, mica and platinum, *J. Am. Chem. Soc.* 40 (1918) 1361–1403.
- [33] K. Yang, L.Z. Zhu, B.S. Xing, Sorption of sodium dodecylbenzene sulfonate by montmorillonite, *Environ. Pollut.* 145 (2007) 571–576.
- [34] Z.H. Li, R.S. Bowman, Counterion effects on the sorption of cationic surfactant and chromate on natural clinoptilolite, *Environ. Sci. Technol.* 31 (1997) 2407–2412.
- [35] P. Reiller, F. Casanova, V. Moulin, Influence of addition order and contact time on thorium(IV) retention by hematite in the presence of humic acids, *Environ. Sci. Technol.* 39 (2005) 1641–1648.
- [36] S. Gangula, S.Y. Suen, E.D. Conte, Analytical applications of admicelle and hemimicelle solid phase extraction of organic analytes, *Microchem. J.* 95 (2010) 2–4.
- [37] D. Xu, X.L. Tan, C.L. Chen, X.K. Wang, Adsorption of Pb(II) from aqueous solution to MX-80 bentonite: effect of pH, ionic strength, foreign ions and temperature, *Appl. Clay Sci.* 41 (2008) 37–46.
- [38] Y.H. Li, S.G. Wang, Z.K. Luan, J. Ding, C.L. Xu, D.H. Wu, Adsorption of cadmium(II) from aqueous solution by surface oxidized carbon nanotubes, *Carbon* 41 (2003) 1057–1062.
- [39] X.L. Tan, M. Fang, C.L. Chen, S.M. Yu, X.K. Wang, Counter ion effects of nickel and sodium dodecylbenzene sulfonate adsorption to multiwalled carbon nanotubes in aqueous solution, *Carbon* 46 (2008) 1741–1750.
- [40] H.J. Wang, A.L. Zhou, F. Peng, H. Yu, J. Yang, Mechanism study on adsorption of acidified multiwalled carbon nanotubes to Pb(II), *J. Colloid Interface Sci.* 316 (2007) 277–283.
- [41] A. Derylo-Marczewska, J. Goworek, A. Swiatkowski, B. Buczek, Influence of differences in porous structure within granules of activated carbon on adsorption of aromatics from aqueous solutions, *Carbon* 42 (2004) 301–306.